Contents list available at IJRED website

International Journal of Renewable Energy Development

Journal homepage: https://ijred.cbiore.id

Research Article

Critical interpretation and analysis to correlate the canopy height to collector diameter ratio for optimized design of solar chimney power plants

Iylia E. Abdul Jamil[a*], Hussain H. Al-Kayiem[b], Sundus S. Al-Azawiey[c], Aseel K. Shyaa[d]

[a]*Mechanical Engineering Department, Universiti Teknologi PETRONAS, 32610 Seri Iskandar, Perak, Malaysia.*

[b]*Air Conditioning and Refrigeration Techniques Engineering Department, Hilla University College, Babylon, Iraq*

[c] *Electromechanical Engineering Department, University of Technology, Baghdad, Iraq.*

[d] *Mechanical Engineering Department, Al-Mustansiryah University, Baghdad, Iraq.*

Abstract. The collector's periphery height determines the entrance size to the solar chimney power plant. There is inconsistency in the published experimental and numerical results on the optimum collector inlet height for different collector diameters. This paper aims to analyze the available data to identify the best collector inlet height-to-diameter ratio and to introduce a design guide for an optimized performance of solar chimney power plants. The experimental data reported in previous works have been clustered and manipulated to produce a comparative argument on the collector inlet height-to-diameter. In addition, a numerical model is developed to support the literature conclusions and to produce further data to decide the optimum collector inlet height-to-diameter ratio. For a 6.6-m collector diameter, four different inlets have been investigated, namely, 0.05, 0.1, 0.15, and 0.2 m. The best performance in terms of air velocity and temperature rise is obtained with the 0.05-m inlet height, where it shows an improvement of up to 35.35% compared to the larger inlet heights. The lower collector inlet height allows a more effective heat transfer from the ground and the collector to the air. It is concluded that the optimum collector inlet height-to-diameter design ratio for solar chimneys with collector diameters larger than 3 m is 0.0075±0.0005. For small-scale solar chimney models with less than 3 m collector diameter, the best collector inlet height-to-diameter ratio ranges between 0.015 and 0.03.

Keywords: solar chimney geometry, canopy height, inlet height-to-diameter ratio

Received: 25th August 2023; Revised: 6th Oct 2023; Accepted: 26th Nov 2023; Available online: 7th Dec 2023

1. Introduction

The Solar Chimney Power Plant (SCPP) technology operates simply by relying on solar energy to heat the air in a solar collector, which then flows along a chimney tower. The SCPP comprises a solar collector, a chimney tower, and a turbine installed at the chimney base to convert the kinetic energy in the heated air to electrical energy. The solar collector is essentially a transparent roof, or canopy, built around the chimney to allow penetration of incident solar radiation on the absorbing ground. The canopy and the solar absorbing ground combined create a greenhouse effect inside the collector. The heated air flows from the solar collector to the chimney base, creating a stack effect and exiting the system at the top of the chimney, as shown in Fig 1. As air exits from the top of the chimney, cool air continuously enters the system through the collector inlet, which is the gap between the ground and the canopy. Installation of a wind turbine coupled in the chimney with a generator will produce electric power. As a green technology, the SCPP appeals to climates with overcast skies as it utilizes diffuse solar radiation. It is also highly suitable for regions with limited access to water as it does not require a cooling water application during its operation. Adding to the advantages, the cost of operation and maintenance of the SCPP is comparatively low due to its simple setup where the turbines and generators are the only moving parts, making it more durable and able to have a long lifecycle. Air, as the heat transfer fluid, operates at low pressure and low temperatures, an additional advantage compared to other solar power technologies that operate under high pressure and high temperature, like concentrated solar power (CSP) technologies.

The first pilot SCPP prototype was successfully constructed in Manzanares, Spain, in 1982. The plant operated for a power output of up to 50 kW between 1986 to 1989, with a chimney height of approximately 194 m and a collector radius of 122 m, While the inlet canopy height is 1.8 m. It is clear that the collector diameter is much larger than the inlet height, and this geometry relation is obvious in all large and small solar chimney (SC) models. Numerous smaller-scale SC prototypes and models have been built and tested worldwide. However, due to the SCPP's low thermal efficiency, construction complexity, and initial cost, none of these setups have a larger collector radius or chimney height than the Spanish plant. The small-scale experimental models have mainly targeted investigations of the parametric relations of the flow inside the SC (Zhou *et al.* 2007; Kasaeian, Heidari, & Vatan 2011; Ghalamchi, Kasaeian, &

* Corresponding author
Email: iylia_0008404@utp.edu.my (I. E. A. Jamil)

https://doi.org/10.14710/ijred.2024.57689
ISSN: 2252-4940/© 2024.The Author(s). Published by CBIORE

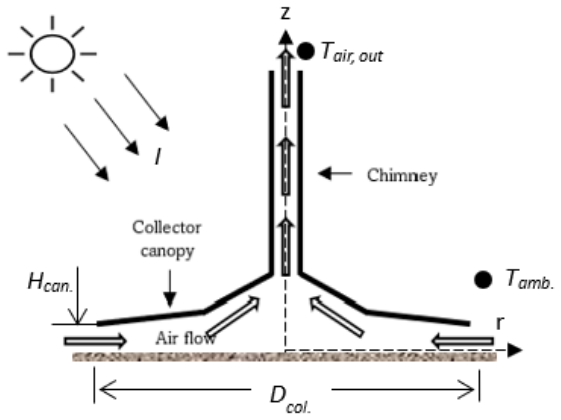

Fig 1. Schematic diagram of the SCPP

Ghalamchi 2015; Guo *et al.* 2016; Lal, Kaushik, & Hans 2016; Ayadi *et al.* 2018), to optimize its overall design (Pasumarthi & Sherif 1998; Ghalamchi *et al.* 2015; Al-Azawiey, Al-Kayiem, & Hassan 2016, 2017), and to investigate potential enhancement methods to the conventional model (Buğutekin 2012; Kalash, Naimeh, & Ajib 2014; Ayadi *et al.* 2018; Aliaga *et al.* 2021; Anbarasi, Rajamurugu, & Yaknesh, 2021).

To increase the attractiveness of the SCPP technology for commercial use, increasing the system efficiency has been the end goal in all ongoing research. Research has shown that large-scale SCPP systems are needed to produce a desirable output (Mullett 2011; Khidhir & Atrooshi 2020). Apart from the overall scale, the design of each component in the system is an important aspect to be optimized. The collector, the chimney, and the turbine are the basic components of the SCPP that are continuously being researched after the decommissioning of the Manzanares plant. Aja, Al-Kayiem, & Abdul Karim (2011); Al-Kayiem & Aja (2016); Too & Azwadi (2016); Guo *et al.* (2019) and Das & Parvathy (2022) provided a comprehensive review of these works until 2022.

It was reported that half of the heat losses in the SCPP happen in the collector (Bernardes, Backström, & Kröger 2009). Many published works focus on studying or improving the canopy, the ground, or both at once. These works can be divided into notable themes, which include analysis of the heat transfers and losses in and around the collector (Pastohr, Kornadt, & Gürlebeck 2004; Larbi, Bouhdjar, & Chergui 2010; Sangi, Amidpour, & Hosseinizadeh 2011; Duffie & Beckman 2013; Ming *et al.* 2013; Niroomand & Amidpour 2013; Pretorius 2004;), enhancement of the ground thermal storage mediums to extend the operability of the plant, and geometry optimization of the transparent collector canopy (Fasel *et al.* 2013; Guo *et al.* 2016; Ismaeel *et al.* 2016; Méndez & Bicer 2021; Pandey, Padhi, & Mishra 2021).

Where geometry is concerned, the detailed optimization work on the SCPP has focused more on the collector diameter and chimney height relationship, along with collector angles and configuration. At the same time, less attention is given to the effect of varying the collector inlet height. The collector inlet height is the entrance to the SCPP, and the inflow of air into the system and any energy transfers and losses are influenced by it. In the Manzanares plant, the collector inlet height is set at 1.85 m, which is backed by a practical reason: it is necessary to allow maintenance vehicles to move under the collector towards the turbine (Too & Azwadi 2016). It is inconclusive how changing the collector inlet height of the plant with a fixed diameter might affect its performance.

This paper focuses on analyzing the effect of varying the inlet height of the collector on the overall SCPP performance based on data from published experimental and numerical works. A new computational study validated by real data is also done to support the analysis. The goal of the work presented here is to propose a design guide in terms of a ratio when determining the optimum periphery height of the collector at the entrance based on any selected collector diameter.

2. Problem Formulation and Initiative

This section discusses in detail the findings from works of literature that focus on the collector inlet height effect on the SCPP performance, both experimentally and numerically.

2.1 Review of Experimental Work with Varying Inlet Height

An operational SCPP requires a large space and high capital cost for construction. Due to this reason, many experimental works conducted are small-scale, with most having a collector diameter of less than or equal to 10 m (Kasaeian *et al.* 2011; Ghalamchi *et al.* 2015; Al-Azawiey, Al-Kayiem, & Hassan 2016; Al-Azawiey *et al.* 2017; Ayadi *et al.* 2018; Anbarasi *et al.* 2021). Furthermore, very few works can be found on the collector inlet height variation based on experiments. This may be reasoned by the additional modification required to the SCPP design to adjust the inlet height while keeping the other geometries constant. Findings from available experiments are analyzed in this section. Several authors described their method of varying the inlet height, which will also be discussed.

Ghalamchi *et al.* (2016) constructed a small setup consisting of a 3-m-tall chimney and a 3-m-diameter collector. The collector is fixed at zero inclination angle, and 40-, 60-, 100-, and 140-mm collector heights have been tested. Data were recorded under the same climatic conditions for four consecutive days. The authors evaluated the performance of the solar chimney based on the air temperature rise and chimney air velocity.

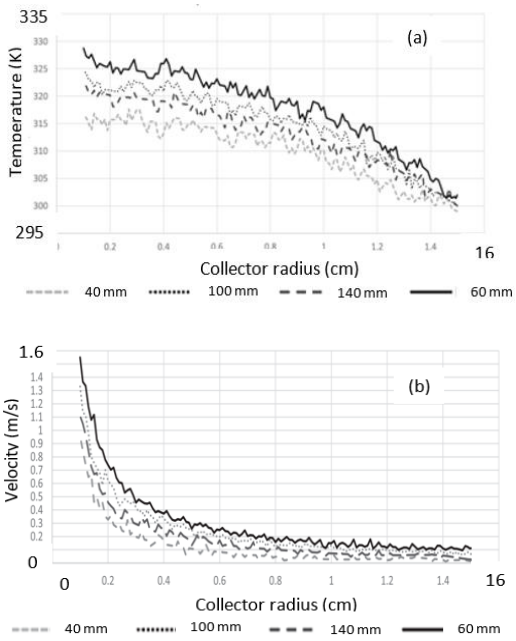

Fig 2 Experimental measurements across the chimney radius for four inlet heights by (Ghalamchi *et al.* 2016), (a) Temperature distribution, (b) Air velocity

The maximum air temperature recorded for the 40-, 60-, 100- and 140-mm inlets are shown in Fig 2a, which translates to temperature rise values of 10.93 K, 23.51 K, 18.35 K, and 16.98 K, respectively. Clearly, the 6 cm collector inlet resulted in the highest temperature rise, which the authors explained is due to a high rate of heat transfer that resulted from the lower air inflow into the system.

Even though the bigger collector heights (100 mm and 140 mm) allow a higher air volume into the system, which could drive flow, the heat transfer rate to the collector's air is insufficient for the high fluid mass. This resulted in less buoyancy created in the air for the bigger inlet height cases. However, no analysis was discussed on the lowest inlet height, 40 mm, recording the lowest temperature rise.

The air velocity results under the collector are shown in Fig 2b. The 60 mm inlet shows the highest velocity at the chimney base at 1.55 m/s, and the 4-cm inlet shows the lowest velocity at 0.91 m/s. This finding is consistent with the temperature rise, where the 6 cm collector inlet showed the best performance for air velocity.

Al-Azawiey *et al.* (2016) designed and constructed a unique SC setup with a variable canopy height, with a collector diameter of 6.0 m and a chimney height of 6.3 m, positioned at a fixed level from the ground. From this experimental setup, four different collector inlet heights were tested: 0.05 m, 0.10 m, 0.15 m, and 0.20 m. Performance was calculated in terms of the mass flow rate of air through the system, temperature rise, and overall system efficiency. The system efficiency is a product of the collector and chimney efficiency under no-load conditions, which are stated as the following:

$$\eta_{collector} = \frac{\dot{m} c_p \Delta T}{I \cdot A_{collector}} \quad (1)$$

$$\eta_{chimney} = \frac{g h_c}{c_p \cdot T_{chimney}} \quad (2)$$

where $\dot{m}$ is the mass flow rate through the chimney, c_p is the air-specific heat at constant pressure, ΔT is the temperature gain in the system, I is solar irradiance, and $A_{collector}$ is the area of the canopy. Chimney height is denoted h_c by and temperature of air inside the chimney is $T_{chimney}$. To calculate the relation, air density, and specific heat values at the temperature range of 300 K – 350 K were determined by empirical correlations.

Under similar ambient conditions, the authors reported ground temperature data with different collector inlet heights. Fig 3 shows that at hours with low solar irradiance, i.e., at the start of the measurements at 8:00 am, the ground temperature values for all the cases are within close range. However, as solar irradiance peaks at noon, the case with the lowest collector inlet, 0.05 m, continually recorded the highest ground temperature until sundown. The highest temperature rise at the ground for collector inlet 0.05 m is 41.4 ºC. Meanwhile, the collector inlet of 0.2 m records the lowest ground temperature rise of 25.2 ºC. This is consistent with the reported findings of Ghalamchi *et al.* (2016), where the low volume of air that can enter the system with a small collector height allows for more effective heat transfer to the available air, therefore increasing the buoyancy effect. As the collector height increases, more air can enter the system, exceeding the capacity of the ground to create buoyancy in the air. As a result, the internal energy of air is lower, thus reducing the stack effect.

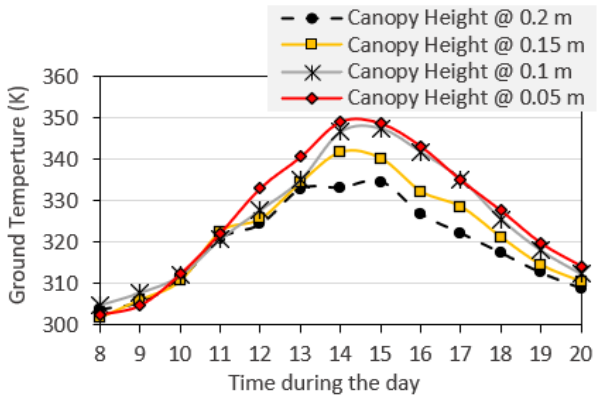

Fig 3 The ground temperature at various canopy heights as measured by Al-Azawiey *et al.* (2016). [Modified with permission]

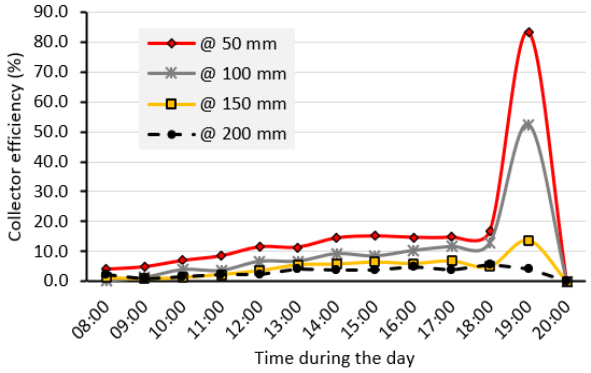

Fig 4 The transient trend of the solar chimney collector efficiency at various canopy heights Al-Azawiey *et al.* (2016). [Modified with permission]

The authors reported the calculated energy transport parameter, $\dot{m} \cdot \Delta T$ for the four cases of collector inlet height: the lowest inlet height of 0.05 m records the highest value of $\dot{m} \cdot \Delta T$, at 0.944 kg·K/s at peak solar irradiance (997.8 W/m^2), while the 0.20 m height records the lowest value of $\dot{m} \cdot \Delta T$, at 0.289 kg·K/s at peak solar irradiance (1042.7 W/m^2). The collector efficiency results presented in Fig 4 affirm that the model with a collector inlet height of 0.05 m records the highest collector efficiency compared to results for canopy heights 0.1 m, 0.15 m, and 0.2 m.

Shyaa (2002) constructed a setup consisting of a 6.5-m tall chimney and a 6-m collector diameter in Baghdad, Iraq. The collector height is adjustable at two points: the center and the periphery, which allows the whole collector to be raised by an even height. Three collector inlet heights are tested: 0.10 m, 0.15 m, and 0.20 m. For each level, measurements are taken for five consecutive days between 12:00 pm to 4:00 pm. The reported solar irradiance levels between these hours averaged between 300 W/m^2 to 500 W/m^2. The author measured the performance of the solar chimney based on temperature readings at various points and velocity at the chimney outlet, and the overall efficiency was calculated for each case. Fig 5a shows that the lowest investigated collector inlet height, 0.10 m, consistently measured the highest air velocity inside the chimney throughout the data collection hours, followed by the collector inlet height of 0.15 m, and the 0.20 m collector inlet height recorded the lowest velocity at all points. The collector efficiency is compared in Fig 5b based on the average performance for each case. The plot shows that when the collector inlet height is 0.10 m, the collector efficiency is highest,

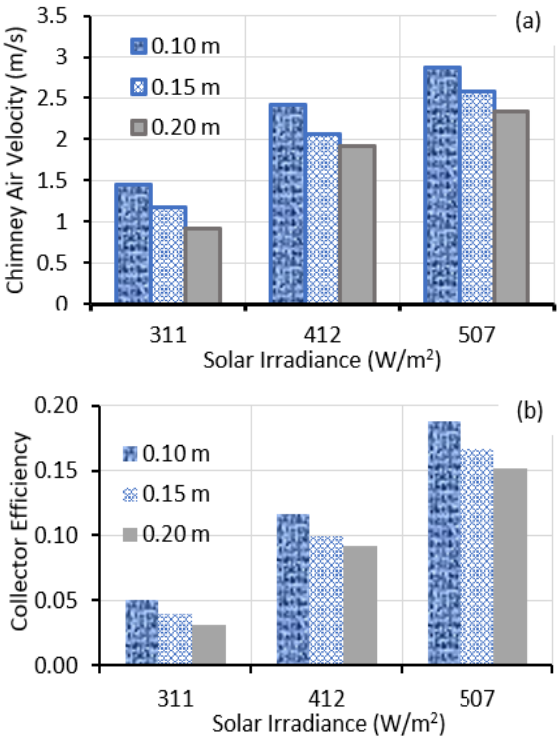

Fig 5 Reported findings for different collector height cases for (a) average air velocity in the chimney and (b) average collector efficiency (Shyaa 2002). [Reproduced with permission]

followed by 0.15 m and 0.20 m. This improvement in collector efficiency is more prominent with increasing solar irradiance.

Kasaeian *et al.* (2011) constructed a 10-m-diameter sloped collector around a 12-m-height chimney to investigate various parameters in the local conditions in Zanjan, Iran. Two collector inlet heights were tested: 5 cm and 15 cm. When the temperature measurements in the 12-m chimney are compared, the temperature rise reported is 22 ºC and 14 ºC for the 5-cm-inlet and 15-cm-inlet, respectively. The authors explained that the higher temperatures observed with the 5-cm-inlet case are due to the lessened wind effects when the collector inlet gap is smaller. This enhances the heat transfer to the air inside the system. The higher temperature rise in the 5-cm-inlet case measures a chimney air velocity of 2.78 m/s, compared to 2.33 m/s in the 15-cm-inlet case.

In modifying the geometry of the collector, experimental investigations are less flexible as most setups are rigid with a fixed diameter, support structure, collector slope angle, and inlet height. Bugutekin (2012) tries to overcome this limitation

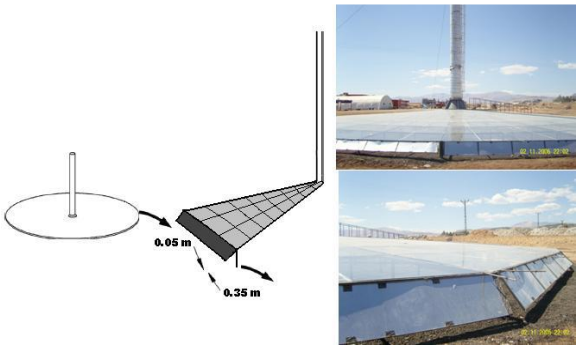

Fig 6 The periphery of the SC is the system inlet for the surrounding air (Bugutekin 2012).

and models the SCPP with a flexible-height periphery around the collector (Fig 6).

To the knowledge of the authors of this publication, this experimental setup by Bugutekin (2012) has the largest scale for testing the effects of varying collector inlet height, with a 17.15-m tall chimney and a 27-m-diameter collector. This experiment tested periphery heights between 0.05 m to 0.35 m. The finding reported that as collector inlet and under the collector rapidly decreased due to the interrupted thermal balance in the system. As the conversion of heat to air kinetic energy decreases, air velocity also decreases, which is consistent with the findings of Shyaa (2002), Kasaeian *et al.* (2011), Al-Azawiey *et al.* (2016), and Ghalamchi *et al.* (2016).

2.2 Comparative Analysis of Experimental Works

A summary of the geometry details from available experimental works is presented in Table 1. From the data, the best ratio of canopy inlet height, H_{can} to collector diameter, and D_{col} can be calculated for each case. The best ratio for Ghalamchi *et al.* (2016) is 0.02; for Al-Azawiey *et al.* (2016) is 0.0083; for Kasaeian *et al.* (2011) is 0.005; for Shyaa (2002) is 0.0167; and for Buğutekin (2012) is 0.00185. The following reasons explain the difference in the best ratio values for each work. Mainly, each work is carried out with a set of fixed geometries, including the collector diameter. Coupled with a range of tested collector inlet height values, the ratio between collector height and collector diameter that are tested differs for each experiment.

In the work of Ghalamchi *et al.* (2016), the best H_{can}/D_{col} ratio is 0.02, which is larger than the other experiments. This is due to the relatively small diameter of the collector, which is 3 m. Lowering the collector inlet height below the best case (from 0.06 m to 0.04 m) has proven disadvantageous to the system

Table 1
Summary of geometry details from experiments, with the range of tested H_{can}/D_{col} ratio and the best equivalent H_{can}/D_{col} ratio reported in each work (Shyaa 2002; Kasaeian et al. 2011; Bugutekin 2012; Al-Azawiey et al. 2016; and Ghalamchi et al. 2016).

Source	Collector diameter	Chimney height	Collector inlet variation method	Tested collector inlet height	Tested H_{can}/D_{col} ratio	Best collector inlet height	Best H_{can}/D_{col} ratio
Shyaa (2002)	6.0 m	6.5 m	Adjustable canopy height	0.10 – 0.20 m	0.0167 – 0.033	0.10 m	0.0167
Kasaeian *et al.* (2011)	10.0 m	12.0 m	Undefined	0.05 – 0.15 m	0.005 – 0.015	0.05 m	0.005
Bugutekin (2012)	27.0 m	17.15 m	Adjustable flap at collector periphery	0.05 – 0.35 m	0.00185 – 0.013	0.05 m	0.00185
Al-Azawiey *et al.* (2016)	6.0 m	6.5 m	Adjustable collector slope	0.05 – 0.20 m	0.0083 – 0.033	0.05 m	0.0083
Ghalamchi *et al.* (2016)	3.0 m	3.0 m	Undefined	0.04 – 0.14 m	0.013 – 0.046	0.06 m	0.02

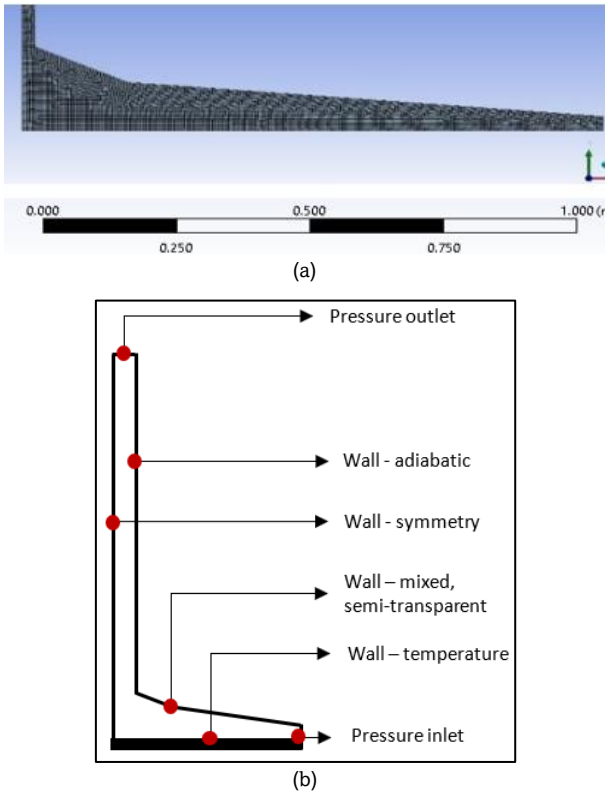

Fig 7 (a) Quadrilateral elements of the model in the collector region and the (b) applied boundary condition of the computational domain.

performance, as reported by the researchers. With such a small gap between the collector periphery and the ground, higher friction losses occur, which reduces airflow into the system.

The experimental results reported by Al-Azawiey *et al.* (2016) showed that the best H_{can}/D_{col} ratio is 0.083, which is the lowest ratio tested in their experiments. It is evident from their results that any larger ratio is disadvantageous to the SC performance, as the higher mass flow of air into the system prevents effective heat transfer from the ground to the air. However, in the Shyaa (2002) experiments, the best ratio is 0.0167 for an inlet height of 0.10 m. Compared to Al-Azawiey *et al.* (2016), which has the same collector diameter of 6.5 m, the H_{can}/D_{col} ratio by Shyaa (2002) is higher. This is because the lowest height tested by Shyaa (2002) is 0.10 m, while Al-Azawiey et al. reduced the height further to 0.05 m.

According to Kasaeian *et al.* (2011), the best H_{can}/D_{col} ratio is 0.005 for a collector inlet height of 0.05 m. Although the best collector inlet height is the same as Al-Azawiey *et al.* (2016), the best ratio is lower in comparison because the collector diameter of Kasaeian *et al.* (2011) is 10 m.

Buğutekin's (2012) experimental results showed that the best H_{can}/D_{col} ratio is 0.00185. This value is the smallest among all reported experiments due to its collector size of 27 m. The collector is 4.5 times larger than that in Al-Azawiey *et al.* (2016) and 2.7 times larger than the model of Kasaeian *et al.* (2011); however, the novel periphery design maintains the smallest collector inlet height of 0.05 m, the same as both Al-Azawiey *et al.* (2016) and Kasaeian *et al.* (2011). This is a crucial finding in the collector design optimization. Hypothetically, if the 0.0083 ratios from Al-Azawiey *et al.* (2016) are followed, the best collector inlet height for Bugutekin's model collector diameter would be approximately 0.22 m. This value is, in fact, within the tested range of collector inlet heights in the experiment (0.05 – 0.035 m). However, results show that the best value is still 0.05 m for the 27-m-diameter collector.

The findings from these experiments suggest that the size of the air inlet plays an important role in the performance of the SC. Researchers agree that a larger scale of the overall system is an important factor in designing a productive SCPP. However, a bigger collector inlet height may disturb the heat transfer between the air and the ground. The design proposed by Bugutekin (2012) has shown that it is possible to have a larger plant while minimizing the adverse effects caused by a larger collector inlet by installing an adjustable flap at the periphery to control the air intake into the system. The adjustable flap allows more flexibility in controlling the size of the air inlet into the system. It effectively reduces the negative impact of ambient crosswinds on the system performance.

In the Manzanares plant, the collector inlet height of 1.85 m (H_{can}/D_{col} ratio = 0.00758) allows passage for maintenance vehicles under the collector to the turbine (Too & Azwadi 2016). However, Bugutekin's (2012) method of reducing the collector inlet height without affecting the overall collector geometry may be explored for a plant of the Manzanares scale.

2.3 Comparative Analysis of Numerical Works with Varying Inlet Height

CFD has proven to be most useful for studying the SCPP, especially in making slight modifications to its design geometry that will not be practical in experimental setups. More published works can be found utilizing CFD to study the effect of changing the collector inlet height on the performance of the SCPP (Ayadi *et al.* 2018; Muhammed & Atrooshi 2019; Anbarasi *et al.* 2021; Mandal *et al.* 2022). The simulation model is validated by real data based on a fixed collector inlet height in all these works. The researchers then modified the simulation model by varying the collector inlet height and performing the calculations. The findings from these works are summarized in Table 2 in terms of the best H_{can}/D_{col} ratio tested in each work.

Mandal *et al.* (2022) modeled the SC with a 2.5-m collector diameter, a chimney height of 6 m, and a collector height ranging between 0.05 m and 0.10 m. The best performance is reported when the collector height is 0.07 m, with a H_{can}/D_{col} ratio of 0.028. The authors stated that a smaller inlet height results in less airflow but higher convection. On the other hand, increasing the inlet's size allows more air volume but with less heat transfer and velocity. The authors also mentioned that an inlet height lower than 0.07 m in their tested model generates a high frictional force, reducing the achieved velocity. It is suggested that a bigger collector area (diameter) and a taller chimney require a larger collector inlet height.

In Ayadi *et al.* (2018) simulation, the SC is modeled with a collector diameter of 2.75 m, a chimney height of 3 m, and a collector inlet height between 0.05 m and 0.2 m. The qualitative results showed that the lowest collector height of 0.05 m, with an H_{can}/D_{col} ratio of 0.0182, creates the highest velocity at the chimney inlet and achieves the highest overall temperature in the SC domain.

Muhammed and Atrooshi (2019) studied 12 groups of variables in collector height for a total of 130 cases. The authors stated that with a larger collector area, reducing friction loss resulting from a low collector is more important. From this work, the best collector inlet height for a range of collector sizes is presented in Table 2.

The suggested H_{can}/D_{col} ratio falls between 0.075 to 0.015 for collector diameters between 20 m to 238 m (Muhammed and

Table 2
Summary of geometry details from simulations, with the range of tested H_{can}/D_{col} ratio (Ayadi *et al.* 2018; Mandal *et al.* 2022) and the best equivalent H_{can}/D_{col} ratio reported in each work (Ayadi *et al.* 2018; Muhammed and Atrooshi 2019; Mandal *et al.* 2022).

Source	Collector diameter	Chimney height	Tested collector inlet height	Tested H_{can}/D_{col} ratio	Best collector inlet height	*Best H_{can}/D_{col} ratio
Ayadi *et al.* (2018)	2.75 m	3 m	0.05 – 0.20 m	0.182 – 0.727	0.05 m	0.0182
Muhammed and Atrooshi (2019)	20 m	12 – 187 m	Unspecified	Unspecified	0.06 m	0.0015
	40 m				0.3 m	0.0088
	60 m				0.35 m	0.0075
	80 m				0.45 m	0.0076
	100 m				0.75 m	0.0075
	122 m				1.0 m	0.0082
	140 m				1.25 m	0.0091
	160 m				1.35 m	0.0085
	200 m				1.5 m	0.0076
	220 m				1.68 m	0.0077
	240 m				1.87 m	0.0079
Mandal *et al.* (2022)	2.5 m	6 m	0.05 – 0.10 m	0.02 – 0.04	0.07 m	0.028

*Best H_{can}/D_{col} ratios are approximated

Atrooshi 2019). The findings from these simulations resemble the outcome of the experiments discussed in section 2.1. With a collector diameter of 3 m or lower, the suggested H_{can}/D_{col} ratio shows values above 0.018, which is larger than the suggested range for bigger collectors. The reason for this is in all cases with small collectors, the collector inlet height tested does not go lower than 0.05 m to avoid undesirable friction losses, and a lower opening would prevent a smooth flow of air into the system. When the collector diameter is increased, the chimney height typically improves the stack effect. The larger overall scale of the SCPP requires a larger entrance of air into the system, as suggested by Muhammed & Atrooshi (2019). For the plant of the Manzanares scale, they suggested that the optimum collector inlet height is 1.0 m, which equals an H_{can}/D_{col} ratio of 0.0041. This value is only 54% of the collector inlet height in the actual plant, 1.85 m. However, as mentioned before, the design of the Manzanares plant is due to practical considerations. The possibility of reducing the inlet size to improve the plant performance by adopting Bugutekin's design has not been implemented.

3. Computational Model Development and Validation

This section presents the numerical work conducted to test the effect of collector inlet height variation at different solar irradiance levels. The main purpose of this simulation is to support the findings from previous publications and to compare the best value for the H_{can}/D_{col} ratio achieved from this simulation.

3.1 Governing Equations

The fundamental governing equations for the simulation are summarized in this section, with explanations of any assumptions made. For the two-dimensional, steady-state model, the continuity equation is given by equation 3.

$$\frac{\delta(\rho u)}{\delta z}+\frac{1}{r}\frac{\delta(r\rho v)}{\delta r}=0 \quad (3)$$

where u and v are the respective velocities in the z and r directions. The momentum and energy equations are given by equations 4, 5, and 6 (Yapıcı, Ayli, & Nsaif 2020).

As the maximum Mach number is much smaller than 1, the assumption that the flow in the model is incompressible is justified. To incorporate the effects of buoyancy, the Boussinesq approximation is adopted, where any changes in density are expressed as a function of temperature.

$$\frac{\delta(\rho uu)}{\delta z}+\frac{1}{r}\frac{\delta(r\rho uv)}{\delta r}=\frac{\delta p}{\delta z}+(\rho-\rho_0)g+2\frac{\delta}{\delta z}\left[(\mu+\mu_t)\frac{\delta u}{\delta z}\right]+\frac{1}{r}\frac{\delta}{\delta r}\left[(\mu+\mu_t)r\left(\frac{\delta u}{\delta z}+\frac{\delta v}{\delta r}\right)\right] \quad (4)$$

$$\frac{\delta(\rho uv)}{\delta z}+\frac{1}{r}\frac{\delta(r\rho vv)}{\delta r}=-\frac{\delta p}{\delta r}+\frac{\delta}{\delta z}\left[(\mu+\mu_t)\left(\frac{\delta v}{\delta z}+\frac{\delta u}{\delta r}\right)\right]+2\frac{1}{r}\frac{\delta}{\delta r}\left[(\mu+\mu_t)r\left(\frac{\delta v}{\delta r}\right)\right]-\frac{2(\mu+\mu_t)v}{r^2} \quad (5)$$

$$\frac{\delta uT}{\delta z}+\frac{1}{r}\frac{\delta(rvT)}{\delta r}=-\frac{1}{\rho}+\frac{\delta}{\delta z}\left[\left(\frac{\mu}{Pr}+\frac{\mu_t}{\sigma_t}\right)\frac{\delta T}{\delta z}\right]+\frac{1}{\rho r}\frac{\delta}{\delta r}\left[\left(\frac{\mu}{Pr}+\frac{\mu_t}{\sigma_t}\right)r\frac{\delta T}{\delta z}\right] \quad (6)$$

The thermal expansion coefficient, β is expressed by equation 7, with the assumption that temperature changes in the system are small.

$$\beta=-\frac{1}{\rho}\left(\frac{\delta\rho}{\delta T}\right)_p\approx-\frac{1}{\rho}\left(\frac{\rho_0-\rho}{T_0-T}\right) \quad (7)$$

The density of air ρ in the flow can be expressed as:

$$(\rho-\rho_0)\approx-\rho_0\beta(T-T_0) \quad (8)$$

where the subscript *0* denotes a pre-set value for density, and this reference density is used in the continuity and energy equations. Equation 8 uses the reference density to calculate the density at varying temperatures in the momentum equation. This model considers the full buoyancy effect, where the flow is motivated by the gravitational force, which is influenced by any change in density.

The radiation energy transfer equation is solved using the Discrete Ordinates (DO) model (ANSYS FLUENT User's Guide, 2013), which solves problems for surface-to-surface radiation involving semi-transparent materials. Equation 9 provides the expression solved by the software.

Table 3
Summary of the simulation model dimensions used in this investigation based on experimental setup.

Parameter	Dimension
Collector diameter	6.60 m
Collector height at the inlet	0.05 m – 0.20 m
Canopy inclination	Inner section 20°, outer section 5°
Chimney height	14.0 m
Chimney diameter	0.15 2 m

$$\nabla.(I_\lambda(\vec{r},\vec{s})\vec{s}) + \nabla.\left((a_\lambda + \sigma_s)I_\lambda(\vec{r},\vec{s})\right) = a_\lambda n^2 I_{b\lambda} + \frac{\sigma_s}{4\pi}\int_0^{4\pi} I_\lambda(\vec{r},\vec{s})\varphi(\vec{s},\vec{s}')d\Omega' \quad (9)$$

In equation 9, a_λ is the spectral absorption coefficient, and σ_s is the scattering coefficient. The solar intensity I_λ is expressed by Equation 10.

$$I_\lambda(\vec{r},\vec{s}) = \sum_k I_\lambda(\vec{r},\vec{s})\Delta I_k \quad (10)$$

where the summation includes all wavelength bands, and direction and position are denoted by $\vec{s}$ and $\vec{r}$, respectively. In this study, the collector material is specified as Perspex with the assumption that it has the same behavior for all wavelength bands.

The performance indicator (PI) for the proposed model is calculated as a product of the temperature gain of air inside the system, ΔT, and the mass flow rate through the system.

$$\dot{m} = \rho A_{ch} V_{ch} \quad (11)$$

$$\Delta T = T_{air.out} - T_{amb} \quad (12)$$

$$P.I. = \dot{m} \cdot \Delta T \quad (13)$$

3.2 Solution Setup

The commercial package ANSYS Fluent 18 is utilized to create the computational model. The domain is built based on an SC plant with a 14-m chimney height and 6.6-m collector diameter in University Teknologi PETRONAS (UTP), Perak, Malaysia. In the experiment, the collector inlet height is set at 0.10 m, while it is varied in the simulation to create four cases: 0.05 m, 0.10 m, 0.15 m, and 0.20 m. The canopy is built at two angles: the inner canopy connects to the chimney base and slopes 20° from the horizontal. In contrast, the outer canopy connects to the inner canopy at 5° from the horizontal and extends for a total of 6.6 m canopy diameter. Only half of the SC domain is modeled to reduce computation time, prescribing the chimney centerline as a symmetry wall. Table 3 summarizes the dimensions of the computational model.

The meshed model is built with 17,651 quadrilateral ele ments after a mesh independence exercise conducted based on the setup described in the next section on four mesh models. This model is chosen based on a difference of less than 1 % in velocity measurements in the chimney when compared to a mesh model with a higher number of elements. Fig 7a shows the meshed model at the collector region in ANSYS.

The computation domain is solved for the steady-state, turbulent, 2-D, and axisymmetric flow, utilizing the equations described in section 3.1. The Boussinesq model is employed to capture the buoyancy effects in the air. In this model, air density is treated as a constant in all equations, except in the momentum equation, where the air density is a function of temperature difference. The inlet and outlet to the solar chimney are prescribed with zero-gauge pressure. No heat transfer is assumed through the chimney wall, which is set as PVC. The canopy is treated as a semi-transparent wall made of Perspex, set with a transmission coefficient of 0.92, and has a thickness of 4 mm (Aurybi *et al.* 2017). The thermal energy transfers through the wall are a mixture of radiation and convection. The discrete ordinate (DO) model for transparent walls is adopted to solve the radiation heat transfer in the simulation domain. The canopy has a thermal conductivity of 0.78 W/m·K to the surrounding. In the solar chimney simulations modeled in 2-D, incident solar radiation through the semi-transparent canopy to the ground is usually treated as heat flux or an internal heat source (Ming *et al.* 2017; Rahimi Larki *et al.* 2021). The ground material is set as black-painted pebbles with an emissivity of 0.95 and an absorptivity of 0.9 (Al-Azawiey & Hassan, 2016). The ground material temperature is prescribed based on experimental values at different levels of solar irradiance. The material properties applied in the model are summarized in Table 4. Fig 7b summarizes the boundary conditions applied to the computational domain.

Table 4
Material properties for simulation.

Physical property	Canopy	Ground	Chimney
Material	Perspex	Black pebble	PVC
Density (kg/m^3)	2700	2640	833
Specific heat (J/kg·K)	840	820	1170
Thermal conductivity (W/m·K)	0.78	1.73	0.19
Transmission coefficient	0.92	0	0
Absorption coefficient	0.06	0.9	0.04
Emissivity	0.9	0.9	0.91

The "SIMPLE" solution scheme is adopted to carry out the computations, and for the convective terms, the second-order upwind scheme is selected. A grid dependency test is carried out by performing the calculations on different grid distributions to obtain the most accurate and efficient solution.

4. Numerical Results and Interpretation

The developed model is validated by comparison against experimental data of the SC plant in UTP. Fig 8 a and b present the validation of the computational procedure by comparison of the velocity and temperature results against experimental results. The results are compared at different levels of solar irradiance. The difference between the experimental and simulation data for air velocity at the chimney base is 4.48%, and for temperature rise is 9.87%. These values are reasonable, and the developed model is accepted as a base for this study.
Four cases are compared based on the validated model. Each case with a different value of collector inlet height: 0.05 m, 0.10 m, 0.15 m, and 0.20 m.

4.1. Comparison Based on Temperature Analysis

Temperature rise is one of the parameters that show the effectiveness of the heat transfer process in the system. It is measured by the difference between air temperature at a point in the system and the ambient. Fig. 11c shows this comparison of temperature gain at the chimney base for all cases of collector inlet height at various levels of solar irradiance. At low solar irradiance of 200 W/m^2, the temperature rise for the 0.05-m, 0.10-m, 0.15-m, and 0.20-m inlets are 1.29 K, 1.23 K, 1.14 K, and 0.49 K, respectively. At a solar irradiance of 1000 W/m^2, the temperature rise for the same cases are 5.19 K, 4.18 K, 4.88 K, and 4.68 K, respectively. The highest temperature rise overall is seen with the lowest inlet height of 0.05 m due to the higher transfer of energy in the greenhouse, while the lowest temperature rise is in the largest inlet height of 0.20 m. This finding is consistent with those reported in previous works, where increasing the inlet height will prevent effective heat transfer between the ground and the air under the collector.

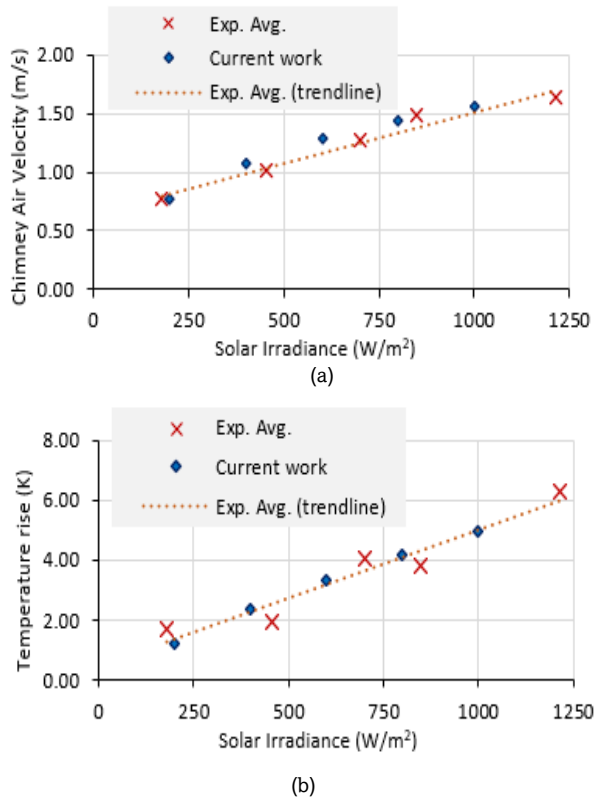

Fig 8 Comparison of simulation and experimental data at different solar irradiance values for (a) chimney air velocity and (b) air temperature rise, taken.

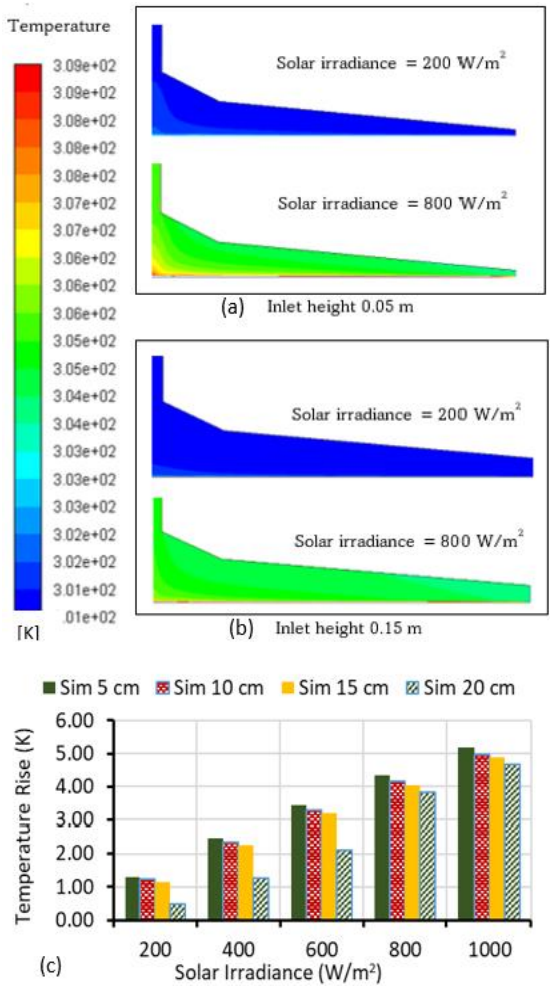

Fig 9 Contours of the temperature field under the collector for the models with (a) 0.05 m inlet height and (b) 0.15 m inlet height at different levels of solar irradiance. (c) Temperature rises in the system for all cases of collector inlet height at different solar irradiance.

The temperature field of air under the collector is visualized in Fig 9 for the cases with 0.05-m and 0.15-m inlet. With the 0.05-m-inlet collector, a higher temperature zone is seen at the collector canter under the chimney, in comparison with the 0.15-m-inlet collector, where the temperature is uniform. This indicates that the thermal energy transfer is more effective in the lower inlet height due to the smaller gap between the canopy and the ground.

4.2. Comparison Based on Velocity Analysis

Air velocity through the chimney is a key parameter in determining the plant's performance. The visualization of airflow in the computational domain is shown as velocity vectors in Fig 10 a and b. In the 0.05-m-inlet model, an increase in the flow towards the chimney is visible, compared to the 0.15-m-inlet model. At low solar irradiance of 200 W/m^2, a stagnant region forms under the collector with the larger inlet. The flow under the collector improves as solar irradiance is increased to 800 W/m^2. However, the larger inlet height reduces the air velocity towards the chimney base, resulting in a lower air velocity through the chimney. For all cases in the simulation, air velocity at the chimney base increases with solar irradiance, as shown in Fig. 10c. At 200 W/m^2, air velocity is lowest in the 0.20-m-inlet model and highest in the 0.10-m-inlet model, with values of 0.564 m/s and 0.781 m/s, respectively. The 0.15-m-inlet model shows a slightly lower value than the 0.10-m, at 0.736 m/s; meanwhile, the 0.05-m-inlet model shows air velocity at 0.773 m/s. The same trend continues as solar irradiance increases, with a reduced gap between the velocity values between the cases. At 1000 W/m^2. Air velocity values for the 0.05-m, 0.10-m, 0.15-m, and 0.20-m-inlet cases are 1.531 m/s, 1.568 m/s, 1.556 m/s, and 1.530 m/s, respectively. The inlet height of 0.10 m results in the highest air velocity value at the chimney base at all the tested solar irradiance levels. These findings, combined with that of the temperature rise, show that even when the temperature rise is the highest, as with the 0.05-m-inlet case, it does not translate to the highest velocity of air through the chimney. The low inlet is effective at retaining the heat in the collector but may also restrict airflow toward the chimney because of the smaller gap between the ground and the canopy. Due to this, the 0.10-m-inlet model allows a smoother flow of air through the collector compared to the 0.05-m-inlet model and gives the best performance in terms of air velocity among all cases.

4.3. Comparison Based on Performance Indicator

The performance indicator, P.I., of the system is measured by mass flow rate and temperature rise as given by equation 13. Fig 11a compares the P.I. value of each model at different levels of solar irradiance. The largest inlet of 0.20 m shows the lowest performance throughout, characterized by the low temperature rise in the system. The smallest inlet of 0.05 m shows the best performance throughout, followed closely by the 0.10 m inlet, then the 0.15 m inlet. Reducing the collector inlet height from

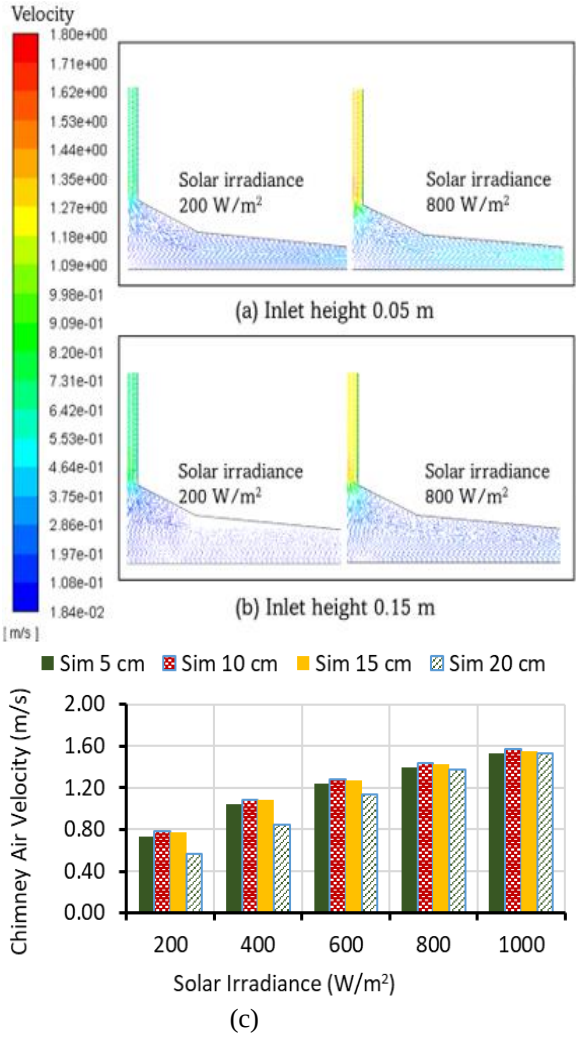

Fig 10 Flow of air in the collector region depicted by velocity vectors for the models with (a) 0.05 m inlet height and (b) 0.15 m inlet height at different levels of solar irradiance. (c) Air velocity in the chimney compared for all cases of collector inlet height at various solar irradiation.

0.20 m to 0.05 m improves the system's performance by 11.12 % when solar irradiance is 1000 W/m^2.

The findings from the numerical investigation presented here are consistent with those from published literature, e.g., Kasaeian *et al.* 2011; Ghalamchi *et al.* 2015; Al-Azawiey, Al-Kayiem, & Hassan 2016; Al-Azawiey *et al.* 2017; Ayadi *et al.* 2018; Anbarasi *et al.* 2021. At collector height 0.05 m, the H_{can}/D_{col} ratio of 0.00758 shows the highest averaged performance, with a P.I. of 0.0919 kg·K/s. Compared with a collector height of 0.10 m and an H_{can}/D_{col} ratio of 0.0152, the improvement is 1.32%. Against the bigger collector inlets of 0.15 m and 0.20 m, with an H_{can}/D_{col} ratio of 0.023 and 0.030, respectively, the improvement is much more significant at 4.91% and 35.35%.

The averaged performance of all cases based on the H_{can}/D_{col} ratio is shown in Fig 11b. A clear decline in performance is seen when the H_{can}/D_{col} ratio is increased past 0.015. The best ratio from this investigation is at 0.00758, while a ratio of 0.0152 shows only a slight reduction in performance, about 1.32%. Increasing the ratio larger than 0.0152 will cause a significant decline in the system performance.

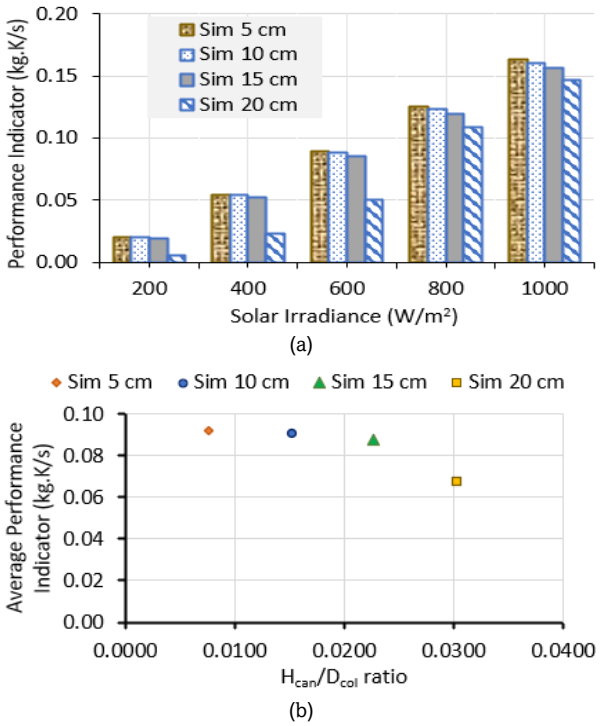

Fig 11 The performance indicator for all collector inlet height cases (a) at different solar irradiance, (b) as average over the day for different inlet heights

4.4. Development of Optimum Inlet-to-Diameter Ratio

The result from the developed numerical model is compared with the findings discussed from reviewed experimental works (section 2.2), reviewed numerical works (section 2.3), and the Manzanares plant. The best H_{can}/D_{col} ratio is plotted against the tested collector diameter from each respective work and presented in Fig 12. In smaller collectors ($D_{col} \leq 10$ m), the best ratio ranges between 0.005 to 0.028, which can be explained by several reasons. First is the limitation on the smallest allowable gap between the collector periphery and the ground to avoid friction losses for the small collectors ($D_{col} \leq 3$ m) seen in the works of Ayadi *et al.* (2018); Ghalamchi *et al.* (2016); and Mandal *et al.* (2022). Second is the different H_{can}/D_{col} range tested, combined with collector diameter in each investigation as analyzed between the works of Al-Azawiey *et al.* (2016) and Shyaa (2002), and (Ghalamchi et al., 2016).

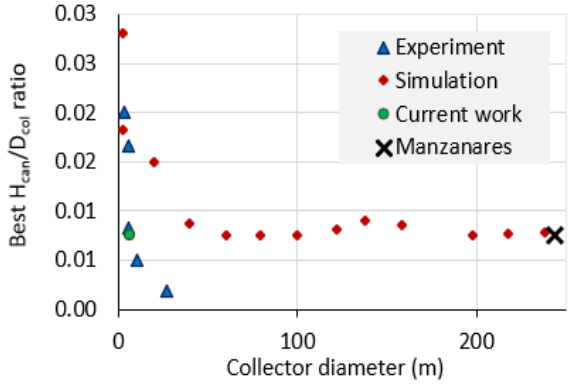

Fig 12 Best H_{can}/D_{col} ratio from literature and the present work based on the tested collector diameter.

The results from Bugutekin (2012), which is for a collector diameter of 27 m, show the lowest ratio of 0.00185, which falls out of the predicted trend. This is justified by the unique collector design adopted, which reduces the inlet height without affecting the overall scale of the collector. For the other cases, the trend shows that the best H_{can}/D_{col} ratio falls between 0.0075 and 0.0091.

Designing the collector of the SCPP is a crucial step in determining its overall performance. The height of the collector at the periphery determines the volume of air that enters the system and affects the mass flow rate through the system, as has been proven and discussed in this work. While there are other parameters of the collector that are influential to the plant performance, like collector slope angle and overall size, it is important to reduce as much uncertainty as possible about its design, and that has been achieved for the collector inlet height in this work. The finding of the optimum H_{can}/D_{col} can be utilized in future research on the SCPP regardless of the plant scale.

5. Conclusions

A comparative analysis has been done to find an optimum ratio of the collector inlet height, i.e., the canopy height above the ground at the inlet, to the collector diameter of the SCPP, H_{can}/D_{col}. In general, the best range of the H_{can}/D_{col} ratio is between 0.007 and 0.008 for a conventional flat or sloped canopy. For smaller experimental prototypes with collector diameters of up to 3 m, the best range of the H_{can}/D_{col} ratio is around 0.015 - 0.03 for a conventional flat or sloped canopy. Numerical and experimental works from published literature show a similar trend of results on the best H_{can}/D_{col} ratio. A new numerical study is done to test the optimum ratio in terms of system performance indicators, $\dot{m}\Delta T$. This study finds that for a collector diameter of 6.6 m, the best H_{can}/D_{col} ratio is 0.0076, followed closely by 0.0152.

Author Contributions: IAJ: Conceptualization, methodology, data collection and curation, formal analysis, writing—original draft, writing – reviewing and editing, HAK: Conceptualization, methodology, experimental investigation, supervision and vetting, writing – reviewing and editing, SSA; experimental investigation, AKS; experimental investigation. All authors have read and agreed to the published version of the manuscript.

Funding: The authors received no financial support for the research, authorship, and/or publication of this article.

Conflicts of Interest: The authors declare no conflict of interest.

References

Al-Azawiey, Sundus S., Al-Kayiem, H. H., & Hassan, S. B. (2016). Investigation on the influnce of collector height on the performance of solar chimney power plant. *ARPN Journal of Engineering and Applied Sciences*, *11*(20), 12197–12201. https://www.arpnjournals.org/jeas/research_papers/rp_2016/jeas_1016_5220.pdf

Al-Azawiey, Sundus S., Al-Kayiem, H. H., & Hassan, S. B. (2017). On the Influence of Collector Size on the Solar Chimneys Performance. *MATEC Web of Conferences*. https://doi.org/10.1051/matecconf/201713102011

Al-Azawiey, Sundus S., & Hassan, S. B. (2016). Heat Absorption Properties of Ground Material for Solar Chimney Power Plants. *International Journal of Energy Production and Management*. https://doi.org/10.2495/eq-v1-n4-403-418

Al-Kayiem, H. H., & Aja, O. C. (2016). Historic and recent progress in solar chimney power plant enhancing technologies. *Renewable and Sustainable Energy Reviews*, *58*, 1269–1292. https://doi.org/10.1016/j.rser.2015.12.331

Aliaga, D. M., Feick, R., Brooks, W. K., Mery, M., Gers, R., Levi, J. F., & Romero, C. P. (2021). Modified solar chimney configuration with a heat exchanger: Experiment and CFD simulation. *Thermal Science and Engineering Progress*, *22*(January), 100850. https://doi.org/10.1016/j.tsep.2021.100850

Anbarasi, J., Rajamurugu, N., & Yaknesh, S. (2021). Optimizing the collector inlet height of a divergent solar tower using response surface methodology. *Materials Today: Proceedings*, *55*, 404–413. https://doi.org/10.1016/j.matpr.2021.10.516

ANSYS FLUENT User's Guide. (2013). Ansys Fluent Theory Guide. In *ANSYS Inc., USA* (Vol. 15317).

Aurybi, M. A., Al-Kayiem, H. H., Gilani, S. I. U., & Ismaeel, A. A. (2017). Numerical assessment of solar updraft power plant integrated with external heat sources. *WIT Transactions on Ecology and the Environment*, *226*(1), 657–666. https://doi.org/10.2495/SDP170571

Ayadi, A., Bouabidi, A., Driss, Z., & Abid, M. S. (2018). Experimental and numerical analysis of the collector roof height effect on the solar chimney performance. *Renewable Energy*, *115*, 649–662. https://doi.org/10.1016/j.renene.2017.08.099

Ayadi, A., Nasraoui, H., Bouabidi, A., Driss, Z., Bsisa, M., & Abid, M. S. (2018). Effect of the turbulence model on the simulation of the air flow in a solar chimney. *International Journal of Thermal Sciences*, *130*(May), 423–434. https://doi.org/10.1016/j.ijthermalsci.2018.04.038

Buğutekin, A. (2012). An Experimental Investigation of the Effect of Periphery Height and Ground. *Journal of Thermal Science and Technology*, *32*(1), 51–58. https://www.acarindex.com/pdfs/687505

Chikere, A. O., Al-Kayiem, H. H., & Abdul Kari, Z. A. (2011). Review on the Enhancement Techniques and Introduction of an Alternate Enhancement Technique of Solar Chimney Power Plant. *Journal of Applied Sciences*, *11*(11), 1877–1884. https://doi.org/10.3923/jas.2011.1877.1884

Das, P., & Velayudhan Parvathy, C. (2022). A critical review on solar chimney power plant technology: influence of environment and geometrical parameters, barriers for commercialization, opportunities, and carbon emission mitigation. *Environmental Science and Pollution Research*, *29*(46), 69367–69387. https://doi.org/10.1007/s11356-022-22623-7

dos Santos Bernardes, M. A., Backström, T. W. Von, & Kröger, D. G. (2009). *Analysis of some available heat transfer coefficients applicable to solar chimney power plant collectors*. https://doi.org/10.1016/j.solener.2008.07.019

Duffie, J. A., & Beckman, W. A. (2013). *Solar Engineering of Thermal Processes, 4th Edition*. https://doi.org/10.1002/9781118671603

Fasel, H. F., Meng, F., Shams, E. & Gross, A. (2013) Cfd Analysis for Solar Chimney Power Plants. *Solar Energy*, *98*, Part A, 12-22. https://doi.org/10.1016/j.solener.2013.08.029

Ghalamchi, Mehran, Kasaeian, A., & Ghalamchi, M. (2015). Experimental study of geometrical and climate effects on the performance of a small solar chimney. *Renewable and Sustainable Energy Reviews*, *43*, 425–431. https://doi.org/10.1016/j.rser.2014.11.068

Ghalamchi, Mehrdad, Kasaeian, A., Ghalamchi, M., & Mirzahosseini, A. H. (2016). An experimental study on the thermal performance of a solar chimney with different dimensional parameters. *Renewable Energy*, *91*, 477–483. https://doi.org/10.1016/j.renene.2016.01.091

Guo, P., Li, T., Xu, B., Xu, X., & Li, J. (2019). Questions and current understanding about solar chimney power plant: A review. *Energy Conversion and Management*, *182*(October 2018), 21–33. https://doi.org/10.1016/j.enconman.2018.12.063

Guo, P., Wang, Y., Li, J., & Wang, Y. (2016). Thermodynamic analysis of a solar chimney power plant system with soil heat storage. *Applied Thermal Engineering*, *100*, 1076–1084. https://doi.org/10.1016/j.applthermaleng.2016.03.008

Guo, P., Wang, Y., Meng, Q., & Li, J. (2016). Experimental study on an indoor scale solar chimney setup in an artificial environment simulation laboratory. *Applied Thermal Engineering*, *107*, 818–826. https://doi.org/10.1016/j.applthermaleng.2016.07.025

Ismaeel, A. A., Al-Kayiem, H. H., Baheta, A. T., & Aurybi, M. A. (2016). Comparative critique of thermal energy storage technique in solar chimney power plants. *International Energy Journal*, *16*(1), 11–24. https://www.thaiscience.info/Journals/Article/RIEJ/10992366.pdf

Kalash, S., Naimeh, W., & Ajib, S. (2014). Experimental Investigation of a Pilot Sloped Solar Updraft Power Plant Prototype Performance Throughout a Year. *Energy Procedia*, *50*, 627–633. https://doi.org/10.1016/j.egypro.2014.06.077

Kasaeian, A. B., Heidari, E., & Vatan, S. N. (2011). Experimental investigation of climatic effects on the efficiency of a solar chimney pilot power plant. *Renewable and Sustainable Energy Reviews*, *15*(9), 5202–5206. https://doi.org/10.1016/j.rser.2011.04.019

Khidhir, D. K., & Atrooshi, S. A. (2020). Investigation of thermal concentration effect in a modified solar chimney. *Solar Energy*, *206*(September 2019), 799–815. https://doi.org/10.1016/j.solener.2020.06.011

Krumar Mandal, D., Pradhan, S., Chakraborty, R., Barman, A., & Biswas, N. (2022). Experimental investigation of a solar chimney power plant and its numerical verification of thermo-physical flow parameters for performance enhancement. *Sustainable Energy Technologies and Assessments*, *50*(August 2021), 101786. https://doi.org/10.1016/j.seta.2021.101786

Mullett, L. B. (2011). *The solar chimney--overall efficiency, design and performance*. International Journal of Ambient Energy, 35-40. https://doi.org/10.1080/01430750.1987.9675512

Lal, S., Kaushik, S. C., & Hans, R. (2016). Experimental investigation and CFD simulation studies of a laboratory scale solar chimney for power generation. *Sustainable Energy Technologies and Assessments*, *13*, 13–22. https://doi.org/10.1016/j.seta.2015.11.005

Larbi, S., Bouhdjar, A., & Chergui, T. (2010). Performance analysis of a solar chimney power plant in the southwestern region of Algeria. *Renewable and Sustainable Energy Reviews*, *14*(1), 470–477. https://doi.org/10.1016/j.rser.2009.07.031

Méndez, C., & Bicer, Y. (2021). Comparison of the influence of solid and phase change materials as a thermal storage medium on the performance of a solar chimney. *Energy Science and Engineering*, *9*(8), 1274–1288. https://doi.org/10.1002/ese3.892

Ming, T., Meng, F., Liu, W., Pan, Y., & Kiesgen de Richter, R. (2013). Analysis of output power smoothing method of the solar chimney power generating system. *International Journal of Energy Research*, *37*(13), 1657–1668. https://doi.org/10.1002/er.2986

Ming, T., Wu, Y., De_Richter, R. K., Liu, W., & Sherif, S. A. (2017). Solar updraft power plant system: A brief review and a case study on a new system with radial partition walls in its collector. *Renewable and Sustainable Energy Reviews*, *69*, 472–487. https://doi.org/10.1016/j.rser.2016.11.135

Muhammed, H. A., & Atrooshi, S. A. (2019). Modeling solar chimney for geometry optimization. *Renewable Energy*, *138*, 212–223. https://doi.org/10.1016/j.renene.2019.01.068

Niroomand, N., & Amidpour, M. (2013). New combination of solar chimney for power generation and seawater desalination. *Desalination and Water Treatment*, *51*(40–42), 7401–7411. https://doi.org/10.1080/19443994.2013.778216

Pandey, M., Padhi, B. N., & Mishra, I. (2021). Performance analysis of a waste heat recovery solar chimney for nocturnal use. *Engineering Science and Technology, an International Journal*, *24*(1), 1–10. https://doi.org/10.1016/j.jestch.2020.11.009

Pastohr, H., Kornadt, O., & Gürlebeck, K. (2004). Numerical and analytical calculations of the temperature and flow field in the upwind power plant. *International Journal of Energy Research*, *28*(6), 495–510. https://doi.org/10.1002/er.978

Pasumarthi, N., & Sherif, S. A. (1998). Experimental and theoretical performance of a demonstration solar chimney model—Part II: experimental and theoretical results and economic analysis. *International Journal of Energy Research*, *22*(5), 443–461. https://doi.org/10.1002/(SICI)1099-114X(199804)22:5<443::AID-ER381>3.0.CO;2-V

Pretorius, J. P. (2004). Solar Tower Power Plant Performance Characteristics. Thesis at the University of Stellenbosch. https://scholar.sun.ac.za/server/api/core/bitstreams/cd87d0e5-4a8b-4260-8649-6b8b91064edf/content

Rahimi Larki, M., Abardeh, R. H., Rahimzadeh, H., & Sarlak, H. (2021). Performance analysis of a laboratory-scale tilted solar chimney system exposed to ambient crosswind. *Renewable Energy*, *164*, 1156–1170. https://doi.org/10.1016/j.renene.2020.10.118

Sangi, R., Amidpour, M., & Hosseinizadeh, B. (2011). Modeling and numerical simulation of solar chimney power plants. *Solar Energy*. https://doi.org/10.1016/j.solener.2011.01.011

Shyaa, A. K. (2002). *Parametric Study of Solar Chimney Performance*. Al-Mustansiriya University.

Too, J. H. Y., & Azwadi, C. S. N. (2016). A Brief Review on Solar Updraft Power Plant. *Journal of Advanced Review on Scientific Research*, *18*(1), 1–25. https://www.akademiabaru.com/doc/ARSRV18_N1_P1_25.pdf

Yapıcı, E. Ö., Ayli, E., & Nsaif, O. (2020). Numerical investigation on the performance of a small scale solar chimney power plant for different geometrical parameters. *Journal of Cleaner Production*, *276*. https://doi.org/10.1016/j.jclepro.2020.122908

Zhou, X., Yang, J., Xiao, B., & Hou, G. (2007). Experimental study of temperature field in a solar chimney power setup. *Applied Thermal Engineering*, *27*(11–12), 2044–2050. https://doi.org/10.1016/j.applthermaleng.2006.12.007